

# The Diffractive Interactions Working Group Summary

H. JUNG<sup>1</sup>, R. PESCHANSKI<sup>2</sup>, C. ROYON<sup>3</sup>

<sup>1</sup> Department of Elementary Particle Physics, Lund University,  
S-22100 Lund, Sweden

<sup>2</sup> Service de Physique Théorique, CE-Saclay, F-91191 Gif-sur-Yvette Cedex,  
France

<sup>3</sup> Service de Physique des Particules, CE-Saclay, F-91191 Gif-sur-Yvette Cedex,  
France

Diffractive interactions represent a lively domain of investigations, as confirmed by the progresses reported during the conference. We summarize the diffractive interactions session and put the new experimental data (section **1**), developments in modeling diffraction (section **2**) and the theoretical relations with Quantum Chromodynamics (section **3**) in perspective.

## 1. HERA and Tevatron on Diffraction

The basis for the investigations on diffraction is provided by a large and interesting set of new experimental data. Indeed, the phenomenon of “hard” diffraction, where a hard probe has been proven to be consistent with a diffractive process, came first as an experimental surprise both at hadron-hadron ( $Spp\bar{S}$ , 88’, Tevatron 95’) and lepton-hadron (HERA, 94’) colliders. It is thus to be remarked that new interesting results have been provided this year by thorough experimental studies at HERA and Tevatron, leading also to a preview on what can be expected from HERA, Tevatron (Run II) and LHC on diffraction in the future.

### 1.1. Diffractive structure function measurements at HERA and QCD fits

The H1 collaboration [1] presented at this conference a new measurement of the diffractive structure function employing the rapidity gap method using the 1997 data representing  $10.6 \text{ pb}^{-1}$  which is 5 times more luminosity than for the previous measurement. In Fig. 1 is presented the new  $F_2^D$  measurement together with the old data of 1994. The kinematical domain is  $6.5 < Q^2 < 120 \text{ GeV}^2$ ,  $0.01 < \beta < 0.9$  and  $10^{-4} < x_{\mathbb{P}} < 0.05$ . Globally a good agreement between the old and the new measurement

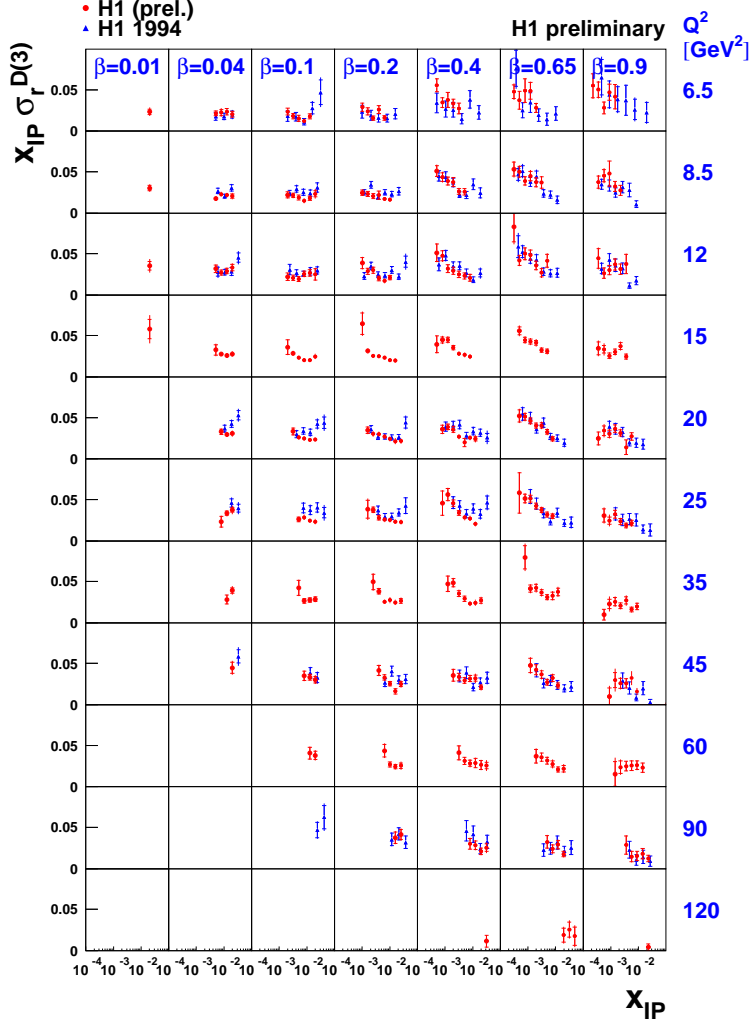


Fig. 1. Comparison on the new (1997) and old (1994) measurements of the proton diffractive structure function from the H1 experiment.

is observed. A few bins show large differences which explain the differences in the QCD NLO DGLAP fit as we will see in the following. A good agreement between the rapidity gap measurement and the Forward Proton Spectrometer data has also been shown [1]. A Regge fit of the new data leads to a new measurement of the pomeron intercept  $\alpha_P(0) = 1.173 \pm 0.018(stat) \pm 0.017(syst)_{-0.035}^{+0.063}(model)$  in good agreement with the

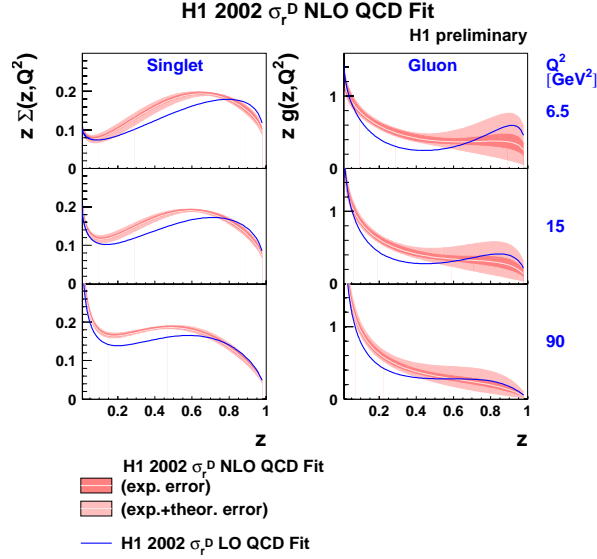


Fig. 2. Quark and gluon density in the pomeron obtained with a NLO and a LO DGLAP QCD fit of the H1 diffractive data.

previous measurement. The growth of  $\alpha_P(0)$  as a function of  $Q^2$  is slower for diffractive events than for inclusive ones [1]. The intercept of the secondary reggeon was fixed to 0.5, consistent with the previous value [2].

The H1 collaboration has also presented a new NLO DGLAP QCD fit of the new 1997 data. The data used in the fit cover  $x_P < 0.05$ ,  $0.01 \leq \beta \leq 0.9$  and  $M_X > 2$  GeV. The latter cut is applied to justify a leading twist approach. Two set of data are used in the fit: the new H1 preliminary data presented at this conference ( $6.5 \leq Q^2 \leq 120$  GeV<sup>2</sup>), and the higher  $Q^2$  data ( $200 \leq Q^2 \leq 800$  GeV<sup>2</sup>) [3]. The quark and gluon distributions together with their errors are given in Fig. 2. The gluon is found to be dominant. The comparison at LO with the previous data is given in Fig. 3 and shows differences for the quark density at low values of  $\beta$ , and for the gluon density over the full range where the gluon is found to be smaller than before. Taking into account the uncertainties (especially of the old fits) the agreement is still reasonable. As we will see in the following, this new QCD fit will have important consequences on diffractive final state predictions and on comparison with Tevatron data. Integrating the parton distributions over the measured kinematic range leads to a determination of the momentum fraction of the color singlet exchange carried by gluons,

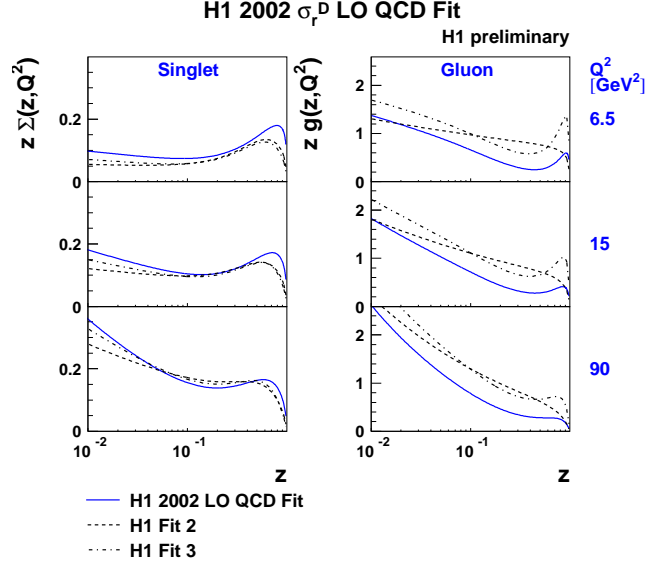


Fig. 3. Quark and gluon density in the pomeron obtained with a LO DGLAP QCD fit of the H1 diffractive data, compared with the result using 1994 data.

which is found to be  $75 \pm 15\%$  at  $Q^2 = 10 \text{ GeV}^2$  [3].

### 1.2. Diffractive and total cross sections

The ratio of diffractive to the total cross section was known to be energy independent, if investigated as a function of  $M_X$  [4]. In this context, progress has been made in understanding also the leading neutron cross sections, as they can be reasonably well described by the one-pion-exchange mechanism and in terms of the pion structure function [5].

In vector-meson ( $V$ ) production the energy dependence of the ratio  $\sigma(ep \rightarrow eVp)/\sigma_{tot}(ep)$  was investigated [6]. The energy dependence of  $\rho$  meson production is found to be the same as for the inclusive cross section for values of  $0.15 < (Q^2 + M^2)/4 < 6.9 \text{ GeV}^2$ , whereas  $J/\psi$  production shows a steeper energy dependence in the same range of  $(Q^2 + M^2)/4$ . In models, where diffraction is directly related to non-diffraction, a steep energy dependence is expected, as observed in the case of  $J/\psi$  production. This observation supports the picture that the pQCD cross section for vector-meson production goes like  $[xG(x, Q^2)]^2$ , with  $xG(x, Q^2)$  being the standard proton gluon density. The observation of no energy dependence in case of the

$\rho$  meson and also for inclusive diffraction implies that the contribution of hard and soft processes is different in diffraction and non-diffraction.

When comparing the ratio with theoretical expectations one should keep in mind, that the inclusive cross section is measured at  $t = 0$  whereas in diffraction normally a range in  $t$  is integrated over, which due to shrinkage in the soft diffractive part, can easily lead to a change of the energy slope of the order of 20 %. If, however, even with a larger lever arm in energy, this ratio stays constant as a function of the energy, much can be learned about the interplay of soft and hard interactions.

### 1.3. Vector meson production

At this conference, new measurements of vector meson ( $\rho$ ,  $J/\psi$ ) production both at large  $|t|$  and at large  $Q^2$  have been presented [7, 8], showing a behavior typical for hard scattering processes, if  $|t|$  or  $Q^2$  is large enough. In photoproduction also  $\psi(2S)$  mesons have been investigated [9] and analyzed in terms of the dipole picture which shows sensitivity to the different wave functions of the  $J/\psi$  and  $\psi(2S)$  mesons. Exclusive  $\rho$  production has been studied at HERMES [10] in terms of the coherence length of the photon. The vector meson studies have also been extended to cover the lightest vector meson, the photon, via the DVCS process [11]. The measurements can be reasonably well described in terms of the approach using generalized parton distributions [12].

Instead of vector mesons with  $C = -1$ , final states with  $C = +1$  can be produced by Odderon exchange. However, no experimental signal for the  $C = +1$  states could be observed [13]. In diffractive dissociation in photoproduction the pomeron intercept  $\alpha_P = 1.127 \pm 0.004 \pm 0.025 \pm 0.046$  has been obtained from a triple Regge analysis [14], which agrees within the errors with the value obtained in diffractive DIS.

### 1.4. Diffraction at Tevatron

#### 1.4.1. Hard diffraction with rapidity gaps

Using the DØ and the CDF detectors, events produced in  $p\bar{p}$  collisions with large rapidity gaps have been investigated at the Tevatron Run I for two center-of-mass energies of 630 and 1800 GeV [15, 16]. The DØ and CDF collaborations have studied the forward and central diffractive dijet productions. The DØ collaboration is requiring two jets with  $E_T > 12$  or 15 GeV in two different pseudorapidity region  $|\eta| < 1$  (central region) and  $|\eta| > 1.6$  (forward region). The fraction of diffractive events in the two kinematical regions for the two center-of-mass energies have been compared to different theoretical predictions. The hard and flat gluon rates predicted by the Monte Carlo are higher than in the data, and the fact that the

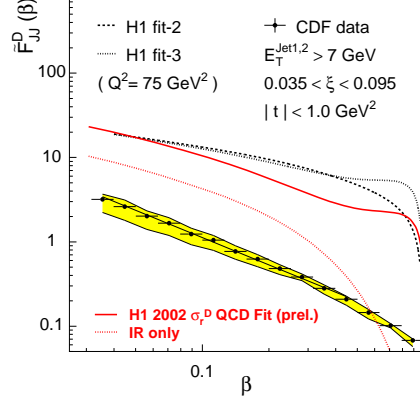


Fig. 4. Comparison of the CDF measurement of the antiproton diffractive structure function with the extrapolation of the H1 measurement using a DGLAP NLO QCD fit. We note a discrepancy in normalization but the shapes seem to be similar.

rates are higher for forward jets than for central ones. This indicates that the data are more compatible with a combination of a soft ( $\sim (1 - \beta)^5$ ) and hard gluon ( $\sim (1 - \beta)$ ) density function in the pomeron. A pomeron made of quarks is also compatible with the data [15]. Contrary to the DØ collaboration who corrects the Monte Carlo prediction and not the data, the CDF collaboration chose to correct the experimental diffractive rates for “rapidity gap acceptance”, defined as the ratio of events with  $\xi$  less than 0.1. This explains most of the differences in diffractive rates published by both experiments. The CDF collaboration has measured the diffractive rates for the Dijet+Gap, Jet+Gap+Jet, diffractive  $b$ , and  $J/\Psi$  production, and they are all in the 1% range [16]. Since the measured single diffractive processes have different sensitivities to the quark and gluon content of the pomeron, it is possible to determine the gluon fraction of the pomeron  $f_g$  which has been found to be  $0.54^{+0.16}_{-0.14}$  to be compared with the HERA result  $75 \pm 15\%$  at  $Q^2 = 10 \text{ GeV}^2$ . [3]

The new result by the DØ collaboration consists in the observation of diffractively produced  $W$  and  $Z$ . The diffractive  $W$  rate is  $0.89^{+0.20}_{-0.19}\%$  (forward:  $0.64\%$ , central:  $1.08\%$ ), and the diffractive  $Z$  rate is  $1.44^{+0.62}_{-0.54}\%$ . This is the first time that an evidence of diffractive  $Z$  production is shown. The CDF collaboration also reports evidence for diffractive  $W$  production, and their rates is  $1.15 \pm 0.55\%$ .

#### 1.4.2. Hard diffraction with tagged protons or antiprotons

The CDF collaboration installed roman pot detectors at the end of Run I to be able to tag the antiprotons in the final state. In leading order, the ratio  $R_{ND}^{SD}$  of single diffractive to non-diffractive dijet production rates is equal to the ratio of diffractive to non-diffractive structure functions of the antiproton. The measurement of this ratio and the knowledge of the antiproton structure function leads directly to a measurement of the diffractive antiproton structure function [16] which can be compared directly to the HERA measurement. Fig. 2 of Ref.[16] shows the measured diffractive structure function in the kinematic region  $|t| < 1 \text{ GeV}^2$ ,  $0.035 < \xi < 0.095$ , and  $E_T^{jet1,2} > 7 \text{ GeV}$ . The comparison between the HERA extrapolation to the CDF kinematical domain and the CDF results is given in Fig. 4 and shows a discrepancy in normalization of a factor 7 to 8 between both experiments. However, contrary to previous results based on previous H1 measurements, the shape of both distributions seems to be quite close [16]. It seems that these results could be interpreted in term of a survival gap probability which does not seem to be kinematically dependent. The knowledge of the secondary reggeon structure function is also not constrained from HERA (the pion structure function is assumed) and can surely influence the comparison between the HERA and Tevatron results. The understanding of diffractive results from HERA and Tevatron together is clearly a theoretical and experimental challenge in the next future, and is fundamental if one wants to understand what diffraction is. This is also important for extrapolating Tevatron results to LHC as we will discuss in the following.

The DØ collaboration has also installed roman pot detectors which will allow to increase notably the possibilities for diffractive measurements at Run II. The DØ Forward Proton Detector (FPD) [17] consists of momentum spectrometers which allow to measure the energies and angles of the scattered proton and antiproton in the beam pipe. Tracks are measured using scintillating fiber detectors located in vacuum chambers positioned in the Tevatron tunnel 20–60 meters upstream and downstream of the central DØ detector. Results using these new detectors are expected for the next DIS conference.

#### 1.4.3. Double-gap soft diffraction

The CDF collaboration presented a study of  $p\bar{p}$  collisions with a leading antiproton and a rapidity gap in addition to that associated with the antiproton [18]. They find that the two-gap to one-gap event ratio is larger than the one-gap to no-gap ratio. It means phenomenologically that the “price” to pay to get a second gap is smaller than the “price” to get one gap. The data are in agreement with the predictions of the gap renormal-

ization approach [18].

### *1.5. Future of diffraction*

#### **1.5.1. Diffractive Higgs production at LHC**

At this conference, the more recent approaches giving predictions for diffractive Higgs cross sections were discussed [19]. We can distinguish between proton-based [20], pomeron-based [21] and soft color interaction based models [22]. These models are compared in detail in Ref [19], and we will only summarize the main results. The proton-based models [20] do not assume the existence of the pomeron and lead to a specific signature where we have the decay products of the Higgs boson in the main detector, the tagged protons in the roman pot detectors and nothing else (exclusive model). This model also predicts the dijet cross sections and thus can be tested directly already at Tevatron. In particular, it leads to a peak in the dijet mass distribution at high values and the Tevatron experiment will be a direct test of this model. The pomeron-based models [21] (inclusive models) assume a pomeron made of quarks and gluons. These models produce a Higgs in the main detector together with the pomeron remnants, and two tagged protons in the roman pot detectors. It is possible to reconstruct precisely the Higgs mass provided one can measure the amount of energy lost in the pomeron remnants [21]. The third set of models based on soft color interaction [22] assumes that diffraction is due to color rearrangement in the final state, and thus does not assume the existence of the pomeron. As shown in Table 1, these models lead to different predictions of the diffractive Higgs production at Tevatron and LHC. All models give low cross sections for the Tevatron, and looking for diffractive Higgs seems to be difficult except for the supersymmetric Higgs, which might increase the cross section notably. At LHC, all models except the soft color interactions give quite high cross section, but still show big differences.

It will be quite important to distinguish between the different models in the near future at the Tevatron. All models can give predictions for diffractive dijet or diphoton production at the Tevatron, and the forthcoming measurements in the next years will allow to distinguish experimentally between the models and to make better predictions for LHC. Another issue is the energy dependence of the survival gap probability which needs to be understood theoretically if one wants to make predictions for LHC [23].

#### **1.5.2. Prospects on experimental facilities**

After more than 10 years after the first results on hard diffraction, the picture of high energy processes becomes clearer. In many aspects diffraction is similar to non-diffractive scattering, and only now with precise mea-



	(1)	(2)	(3)	(4)
H $\sim$ 120 GeV, Tevatron	0.3	3.	22	$1.2 \cdot 10^{-3}$
H $\sim$ 120 GeV, LHC	14.	3600.	3219.	0.2
H $\sim$ 160 GeV, LHC	5.5	1460.	2100.	?

Table 1. Number of events for  $10 \text{ fb}^{-1}$  for diffractive Higgs production for different models (exclusive Higgs production (1), inclusive Higgs production in the factorizable (2) and non factorizable (3) cases, soft color interaction model (4)).

collider	energies [GeV]	$\sqrt{s}$ [GeV]	lum [ $/\text{sec}/\text{cm}^2$ ]
EIC	$E_e = 3 - 10, E_p \sim 30 - 250$	$\sim 20 - 100$	$\sim 10^{33} - 10^{34}$
HERA III	$E_e \sim 30, E_p \sim 820 - 920$	$300 - 330$	
HERA	$E_e = 250 - 500, E_p \sim 1000$	$1000 - 1414$	$\sim 10^{30}$

Table 2. Possible future collider options at ELECTRON ION COLLIDER (EIC), HERA III and THERA.

surements, deviations from the simple expectations are observed. However, more investigations are needed to substantiate such observations. With the upgraded HERA machine a substantial increase in luminosity is still expected, and with the installation of the new very forward proton spectrometer (VFPS) exciting new results can be expected [24].

The understanding of diffraction seems to act as a key to the understanding of the structure of the proton, be it in terms of confinement or in terms of high parton densities and self interaction leading to saturation, or simply in terms of the small  $x$  evolution of parton densities. Given the importance of understanding QCD as a whole, several future collider options are presently discussed where these and other questions could be answered [25] (see Tab. 2).

## 2. Modeling Diffraction

Several theoretical approaches to calculate total cross sections in diffraction exist. However, modeling the hadronic final state of diffractive processes in detail is much more complicated compared to non-diffractive scattering, because the color connection of the produced partons might influence on the production of the rapidity gap or as in the case of charm, the  $c \rightarrow D^*$  fraction might be different compared to the inclusive case, since also  $c\bar{c}$  bound states, like  $J/\psi$  might be produced. In addition multi-gluon emissions in the QCD cascade, initial and final state parton showers or color dipole emissions, have to be modeled properly, since they can easily affect the hadronic final state as well as the formation or destruction of the

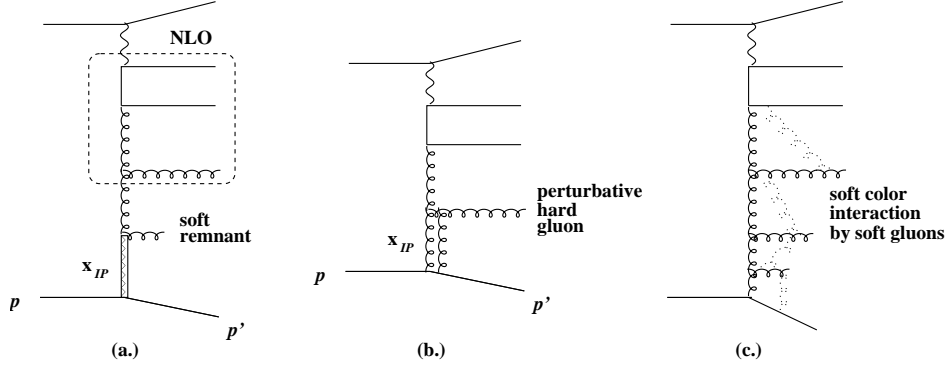


Fig. 5. Schematic diagrams for diffractive  $ep$  scattering in the *resolved pomeron model* (a.), in the *pQCD 2 gluon model* (b.) and in the *SCI* approach (c.). In (a.) a typical tree level  $\mathcal{O}(\alpha_s^2)$  diagram is shown.

rapidity gap.

### 2.1. Models

The following three approaches, applicable to diffractive scattering in  $ep$  and  $p\bar{p}$  processes, are included in full hadron level Monte Carlo programs:

- The *resolved pomeron model* (Fig. 5(a.)) either based on the Ingelman-Schlein ansatz with the additional assumption of Regge factorization ( $IP$  - flux), or in the more general formulation applying the factorization theorem of Collins.
- The *perturbative 2-gluon* picture [26] (Fig. 5(b.)) either in its realization in the wave function approach, in the dipole model or in the  $k_t$ -factorization approach.
- The *soft color interaction model* [22] (Fig. 5(c.)) and its extension to the generalized area law model.

Please note, that we have chosen for practical reasons short names to identify the different approaches.

#### 2.1.1. Resolved pomeron model

This approach has its origin in the Ingelman-Schlein model, which says, that diffraction is mediated by the pomeron  $IP$  which behaves like a particle and consists of partons, which can be described by parton density functions (pdf) evolved with the DGLAP evolution equations. Hard scattering processes, like jet - or heavy quark production occur according to the same

hard scattering matrix elements as known from standard  $ep$  and  $p\bar{p}$  scattering. In general, it is enough to define diffractive parton density functions  $f^D(\xi, x_P, t; Q^2)$ , without making any assumption about the pomeron.

Collins showed, that diffractive processes, induced by scattering of a (direct) photon, can be factorized into these diffractive pdf's  $f^D(\xi, x_P, t; Q^2)$  and hard scattering coefficient functions, as known from standard QCD processes:

$$d\sigma = \sum_i \int d\xi f^D(\xi, x_P, t; Q^2) d\hat{\sigma}_i \quad (1)$$

up to corrections that are power suppressed in  $Q$ , with  $\xi$  being the fractional momentum of the struck parton relative to the pomeron,  $\xi = x/x_P$ .

Important is the statement, that the factorization theorem is valid *only* for direct photon and leading  $Q^2$  contributions. Nothing is said about the relative size of the non-leading contributions, and whether they are larger or smaller compared to inclusive processes. This factorization theorem is expected not to be valid in the case of  $p\bar{p}$  or resolved photon interactions.

The diffractive parton densities  $f^D(\xi, x_P, t; Q^2)$  are determined by LO or NLO DGLAP fits to the diffractive structure function  $F_2^{D(3)}(\xi, x_P; Q^2)$ . With NLO diffractive parton densities also NLO order programs might be used for diffractive di-jet production as well as for diffractive charm. However, it is necessary to treat the *pomeron remnant* properly, as the details affect the formation of the rapidity gap, which often forms the basis for the calculation of  $x_P$  (see Fig. 5). In the case of charm production, additionally one has to treat properly the formation of one or two  $D^*$ -mesons and also of bound  $c\bar{c}$  states, which are not covered by applying naively the fragmentation functions.

### 2.1.2. Two-gluon approach

Diffractive final states, which consist of hard jets or heavy quarks (without soft remnants) can be fully perturbatively calculated because the hard scale which allows the use of pQCD is provided by the large transverse momenta of the jets, and the Pomeron exchange is modeled by the un-integrated gluon density of the proton. Recently, full perturbative calculations were done for  $ep \rightarrow e' q\bar{q} p$  and  $ep \rightarrow e' q\bar{q}g p$ , where  $q$  can be a light or heavy quark [26] (see Fig. 5). This approach provides a natural connection to non-diffractive scattering as the same un-integrated gluon density is used, without any new parameters.

These perturbative calculations have been implemented in the RAPGAP Monte Carlo generator, supplemented with final state parton showers and full hadronization. Recently, also different approaches to parameterize the un-integrated gluon density were published, which are applicable also to

the region  $k_t \rightarrow 0$ . This region is important in the calculations, as the un-integrated gluon density appears inside an integral over an internal loop.

### 2.1.3. Soft Color Interaction model

The soft color interaction model (SCI) and the generalized area law model (GAL) were developed under the assumption that soft color exchanges give variations in the topology of the color strings such that different final states could emerge after hadronization, e.g. with and without rapidity gaps or leading protons. The same hard scattering processes as in non-diffractive scattering are used, with the same non-diffractive parton density functions. In the SCI model an explicit mechanism is applied to exchange color between the emerging partons, in the GAL model color is exchanged between the strings. The probability for the soft color exchange to happen, is a free parameter which has to be determined from experiment.

The SCI and GAL models are successful in describing  $F_2^{D(3)}$  as well as diffractive jet production at the Tevatron [22].

However, it has been argued [27], that using the standard DGLAP pdfs of the proton together with DGLAP parton showers to describe diffraction might be problematic. Especially in the forward region of  $\eta \sim 3$ , which is often used to select diffractive events, and which corresponds to  $x_P \leq 0.05$ , the standard DGLAP approach already fails to describe non-diffractive processes, like forward jet production. Diffractive scattering could be sensitive to small  $x$  effects in the parton distribution functions, as predicted by BFKL or CCFM.

## 2.2. What is new ?

It is interesting to note, that all three approaches and models to describe and understand diffractive scattering have been basically presented already in 1995, where the first detailed measurements of the diffractive structure function  $F_2^{D(3)}$  has been presented.

Besides the measurements of vectormeson production and  $F_2^D$  [4, 1] with the pdf fits [3], new measurements of charm production have been performed [28] and compared to predictions using diffractive parton densities.

Now having new and more precise measurements on charm and jets available, tests of the factorization theorem can be performed as well as more detailed investigations of the structure of the diffractive hadronic final state. The discrepancy in description of di-jet and charm is suggestive for mechanisms of factorization breaking and deviations from the DGLAP picture. As discussed below, the 2-gluon picture could provide an explanation of these effects. However one has to keep in mind, that the errors both on

the data and also on the diffractive pdfs are still too large to draw final conclusions.

### 2.3. Factorization tests

One of the most important issues in diffraction is the universality of diffractive parton density functions:

- To which extend is the factorization theorem in deep inelastic diffraction satisfied ? Is it similar to non-diffraction or are there differences?
- Are pdf's obtained in  $ep$  scattering applicable to  $p\bar{p}$  scattering ?

To answer these questions, the diffractive parton densities have to be determined precisely. Then these pdf's can be used in other processes to compare predicted cross sections with the measured ones.

#### 2.3.1. Factorization tests at HERA

The diffractive parton densities are used in the *resolved pomeron* approach to calculate inclusive diffractive cross sections as well as the cross sections for jet and charm production. For practical reasons it is important to perform all calculations within the same framework and program, as different extrapolations from the measured to the hadron or parton level cross section might introduce additional uncertainties. Such extrapolations can only be performed properly by the use of full hadron level Monte Carlo generators, and different approaches within the same framework help to estimate the model uncertainties.

In general the MC predictions obtained in the *resolved pomeron* approach agree very well with the measurements, as shown in detail in [29]. Using the (old) H1 fit2 as a parameterization of the diffractive parton densities, di-jet production in diffractive DIS [30] is well described, if resolved virtual photon contributions are included to simulate the  $O(\alpha_s^2)$  (NLO) corrections. However, using the same parameter set (and the same Monte Carlo event generator) the predicted cross section for charm production [31] overshoots the data. A new and precise measurement of charm production in diffractive DIS, performed by ZEUS, has been presented at this conference [28]. Using the H1 fit2 the Monte Carlo predictions overshoot the data significantly, whereas with the new set of diffractive pdf's, diffractive charm production in deep inelastic scattering is reasonably well described (Tab. 3). In Fig. 6 we show the comparison of the ZEUS diffractive charm measurement with the predictions from the resolved pomeron model using the old and the new diffractive pdf's obtained by H1 [2]. However, applying the same diffractive pdf's to diffractive di-jet production, the predicted cross section is smaller

	H1 fit2	New H1 fit
H1	$0.67 \pm 0.15 \pm 0.15$	$1.23 \pm 0.27 \pm 0.28$
ZEUS	$0.63 \pm 0.07^{+0.04}_{-0.08} \pm 0.03$	$1.31 \pm 0.12^{+0.08}_{-0.16} \pm 0.05$

Table 3. The ratio  $R^{D^*} = \sigma(\text{data})/\sigma(\text{MC})$  for diffractive charm production of H1 and ZEUS [28] obtained from the H1 fit2 and the new H1 fit [3] presented at this conference.

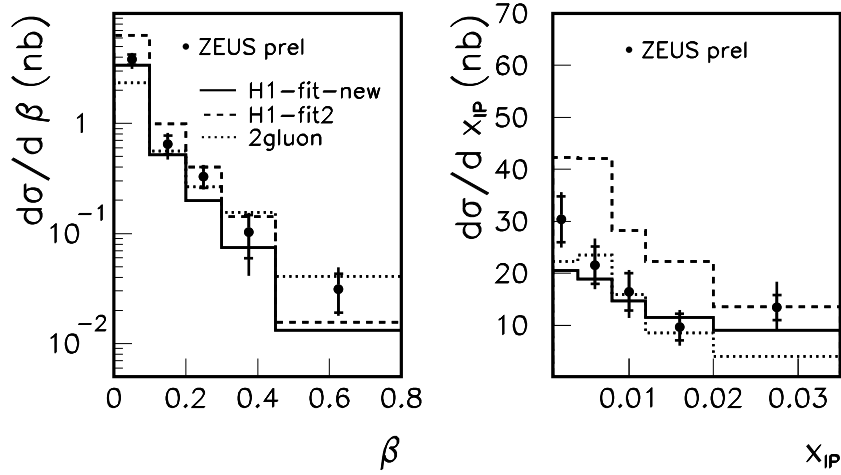


Fig. 6. The cross section of charm production in deep inelastic diffraction as measured by ZEUS[28] compared to the prediction from RAPGAP using the old and the new diffractive pdf's as obtained by H1 [2]. Also shown is the prediction of the perturbative 2-gluon approach with the unintegrated gluon from the saturation model.

compared to the H1 measurement [30]. It is suggestive that even with the new pdf set a difference is observed in the description of diffractive final state processes.

### 2.3.2. Factorization breaking at HERA?

The difference in description of diffractive di-jet and charm measurements within the *resolved pomeron approach* might be a possible sign for factorization breaking, as the corresponding quantities are well described in non-diffractive  $ep$ -scattering. A possible mechanism to explain factorization

breaking between diffractive charm and di-jet production is provided by the perturbative calculation of 2 gluon exchange processes: with a reasonable choice of the un-integrated gluon density, both charm and di-jet production can be described using the same set of parameters. This becomes understandable since so called *non- $k_t$ -ordered* gluon emissions contribute differently to the di-jet and charm sample. In the kinematic range of the analysis, the perturbative 2-gluon calculation [26] (as implemented in RAP-GAP) yields much more events having a gluon with transverse momentum larger than those of the quarks:  $\sim 30\%$  for diffractive di-jets and  $\sim 15-17\%$  for diffractive charm, compared to 2 - 3% obtained in the resolved pomeron mode, depending on the choice of the factorization scale  $\mu^2$ .

The calculation has been previously compared with the measurement of diffractive di jet production, and reasonable agreement has been found in the region of  $x_{\mathbb{P}} < 0.01$ , if the transverse momenta of all partons are required to be larger than  $k_t \gtrsim 1.5$  GeV. Especially the gluon in the  $q\bar{q}g$  process is found to be hard, in contrast to the expectation in the resolved pomeron model, where this gluon should appear as a soft pomeron remnant. As presented in this workshop, the perturbative calculation has also been compared with the measurement of diffractive charm production [26, 28]. For both the H1 and ZEUS measurement reasonable agreement has been found using the same cutoff of  $k_t \gtrsim 1.5$  GeV for the gluon transverse momentum. A comparison with the new charm measurement of ZEUS is shown in Fig. 6.

The above considerations show, that a detailed simulation of the hadronic final state in diffraction is inevitable when going beyond total cross section calculations.

### 2.3.3. Factorization tests: HERA versus Tevatron

As already mentioned, the measurement of diffractive di-jet production at the Tevatron compared to the prediction using diffractive pdf's obtained from HERA can be used directly to test the factorization hypothesis.

CDF [16] has measured the measured diffractive structure function in the kinematic region  $|t| < 1$  GeV<sup>2</sup>,  $0.035 < \xi < 0.095$ , and  $E_T^{jet1,2} > 7$  GeV. The comparison between the HERA extrapolation to the CDF kinematical domain shows a discrepancy in normalization of a factor 7 to 8 between both experiments, see Fig.(4). However, contrary to previous results [16] based on old H1 diffractive pdfs, the shape of both distributions seems to be quite close [16, 3]. It seems that these results could be interpreted in term of a gap survival probability which does not seem to be kinematically dependent.

However, the observation of non-factorization at  $p\bar{p}$  does not come as a surprise as already in the proof of the factorization theorem it has been

noted that this only applies to direct photon interactions.

#### 2.3.4. Global fits of HERA and Tevatron data

An attempt to fit together HERA and Tevatron data has been performed in Ref. [32]. It was found that it is impossible to fit both sets of data together even by letting free the normalization between both experiments. Unfortunately, this study has been performed using the old published 1994 H1 diffractive structure function data, and it would be worth to redo it using the preliminary 1997 data, since they lead to different quark and gluon densities in the pomeron. A gluon density has also been extracted directly from CDF data and found to be more proton-like, with a softer value of the intercept, than the diffractive gluon density at HERA [32].

It is interesting to note, that in contrast to single diffraction mention above, the mass fraction measured in double diffractive events by the CDF collaboration is compatible with the HERA gluon density and not with a proton-like structure function. It seems that double diffraction at Tevatron is harder than single diffraction. More data from Tevatron are needed to do more studies related to the dijet mass fraction, which will happen very soon with the start of Run II.

### 3. Diffraction and QCD Theory

There are several connections with basic problems in QCD raised by experimental and phenomenological studies on diffraction, but they are kind of subtle. Indeed, “hard diffraction” being a superposition of a short space-time interaction at weak coupling (at the hard  $\gamma^*$ , dijet, Higgs,...vertex) with a typically soft process at strong coupling (at the soft vertex with the ingoing proton or antiproton), it is highly non trivial to formulate it in fundamental terms. On the other side of the same coin, hard diffraction may represent a new route to theoretical progress in the interface between soft and hard QCD, and thus for a more complete, and presently yet unknown, formulation of the theory.

#### 3.1. Small- $x$ : questions and progresses

One important theoretical aspect where diffraction can teach us something is the never-ceasing discussion on the physical relevance (or not) of the BFKL type of evolution equation. Indeed, diffractive processes represent a good opportunity of so-called “one-scale” configurations, where the “BFKL logs” are favored w.r.t. the usual DGLAP evolution. This is well illustrated in the study of vector meson production. Deeply virtual Compton scattering adds a new aspect of the problem by the comparison of QCD dipole models



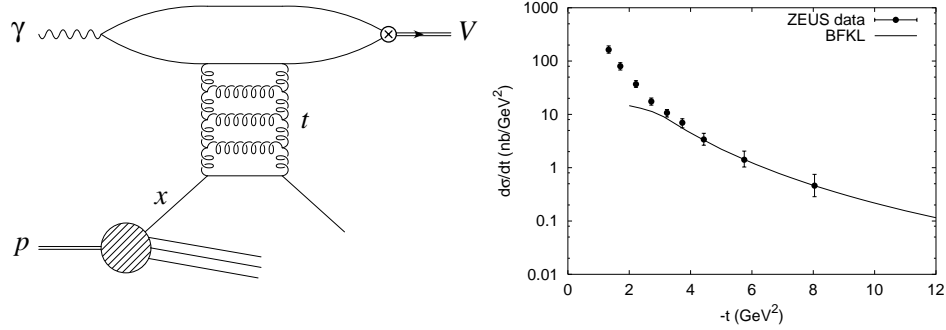


Fig. 7. Feynman graphs and differential cross-section for the process  $\gamma p \rightarrow \rho X$  at large  $t$  (from [33]).

(neighboring BFKL evolution) with Generalized pdf's (extending DGLAP evolution).

### 3.1.1. Is BFKL “seen”? : Vector meson production

Diffractional vector meson production at large momentum transfer  $t$  accompanied by proton dissociation is a good laboratory for studying resummation of perturbative QCD effects in color singlet exchange reactions. Indeed, this is a one-hard-scale process which is expected to be described by the non-forward BFKL equations. However, the usual leading  $\log 1/x_{Bj} \sim Y$  approximation ( $Y$  is the rapidity gap interval), corresponding only to the leading “conformal spin”  $n$  of the expansion of the BFKL equation's solution, fails to reproduce the data. In [33], it is shown that the inclusion of the whole  $n$  expansion gives a good description of data, see Fig. 7, and also a reasonable one of spin density matrix elements. It is not clear, however, how the next-to-leading  $\log x_{Bj}$  contribution, which is known to be large at least at  $t = 0$ , would modify the conclusions. An argument is that the simplest Feynman graph in Fig. 7, *i.e.* the 2-gluon exchange, includes already an all- $n$  expansion. More work is deserved in this interesting direction, including large  $t$  processes at Tevatron. A puzzle to be solved is the value of the strong coupling constant in the cross-section prefactors, which ought to be *non running* for phenomenological applications, while common wisdom would expect an improvement with usual running behavior.

At smaller momentum transfer and in total  $\gamma^* p \rightarrow V p$  cross sections, the hard scale is provided by  $Q^2$ . In BFKL physics, the coupling to the proton is *via* the un-integrated gluon distribution, where track is kept of the transverse momentum of the gluon. This “ $k_T$ -factorization” property

allows to relate the studied processes to the proton structure function in the BFKL formalism. In [34], both non-perturbative and perturbative QCD contributions to the un-integrated gluon distribution have been considered, where soft and hard components are strongly separated. The comparison with cross-sections shows discrepancies while ratios, *e.g.*  $\sigma(\phi)/\sigma(\rho)$  are in better shape. One remark is that progress on the various determinations, models and theoretical properties of un-integrated gluon distributions are highly required in this field.

### 3.1.2. Dipoles or Generalized pdf's? : $\gamma^* p \rightarrow \gamma p$

Color dipole models accommodate rather easily the description of DVCS ( $\gamma^* p \rightarrow \gamma p$ ) processes. In [35], for instance, two different models for the dipole-proton cross-sections, one with saturation included (MFGS) and one without (FKS) give good predictions for DVCS data, see Fig. 8, based on non-perturbative inputs for *other* processes. On the other hand, the approaches based on NLO QCD evolution equations [36], which are more solid on a theoretical point of view, seem however to depend much [12] on the non-perturbative input for the *same* process, even if good candidates have been found. On a theoretical ground, it will be worthwhile to understand better the connections between the two approaches, the former being “*s*-channel” and the latter “*t*-channel” oriented. DVCS can then be a good laboratory for the much discussed comparison of “*s*-channel” and “*t*-channel” models. The comparison between elastic and inelastic diffraction has been wisely

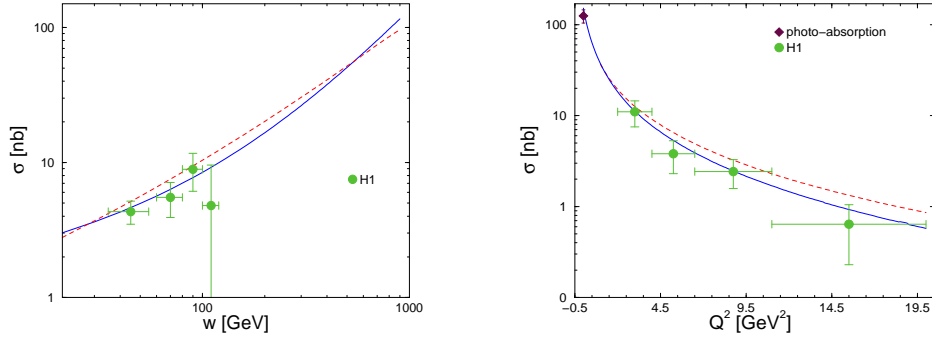


Fig. 8. The energy (at  $Q^2 = 4.5 \text{ GeV}^2$ ) dependence and  $Q^2$ -dependence (at  $W = 75 \text{ GeV}$ ) of the photon level DVCS cross-section, FKS (solid line) and MFGS (dashed line) (from [35]).

advocated to be important for the validity of dipole models. A variant of the model, motivated by generalized vector dominance [37], is shown to lead to a specific geometrical scaling prediction for elastic diffraction and

a good prediction for the longitudinal (high  $\beta$ ) part of inelastic diffraction, while the transverse photon polarization requires higher spin components of the hadronic states. More work disentangling the various versions of dipole models is certainly deserved in the near future. Another type of dipole model has been advocated [38], which relies on the introduction of instantons to describe the soft QCD regime of the dipole-proton diffractive coupling. All this emphasizes the importance of a good understanding of the dipole-proton cross-section both in the perturbative and non-perturbative regimes.

A relevant point for the discussion is the amount of higher-twist with respect of leading twist contributions in diffractive processes. It is known that the “ $s$ -channel” naturally contain larger higher-twist components than “ $t$ -channel” ones. Nuclear shadowing has been suggested [36] to give experimental separation between these two options by looking to nuclear gluon pdf’s through the analysis of  $F_{2A}/AF_{2N}$  at very small  $x_{Bj}$  when possible. Note also [39] the interest of double spin asymmetries in diffractive  $Q\bar{Q}$  production.

### 3.2. Smaller- $x$ : Saturation, myth or reality?

The question of *saturation* has been a major problem discussed in the conference. For  $x_{Bj} \rightarrow 0$ , the growing number of gluons of fixed size  $1/Q$  in the wave-function of the proton becomes high enough that new multiparton interaction occurs. These effects modify the evolution equations by the addition of non-linear terms and even may lead to a new phase of QCD.

#### 3.2.1. Has Saturation already been seen at HERA?

Despite the existence of an elegant and inspiring model of saturation [40], there is not yet any compelling evidence of saturation in inclusive structure function data. Hence it is of primary importance to look for model-independent investigations on saturation with less inclusive data at HERA.

This has been proposed in [41] using diffractive  $\rho$  production cross-section on a proton as a function of  $t$ . The method is to extract the  $S$ -Matrix elements  $S(x_{Bj}, r_Q, b)$ , where  $r_Q$  is the mean dipole size probed by the  $\rho$  wave-function and  $b$  is the impact parameter of the reaction. Interestingly enough, see Fig. 9, perturbative saturation (likely to be reached when the interaction probability  $1-S^2$  is large while  $1/Q$  remains small) seems to be relevant at small  $b$ . This might be interpreted as a first experimental evidence for saturation [41]. Complementary confirmation is highly deserved for this first experimental evidence for saturation at small  $b$  at HERA.

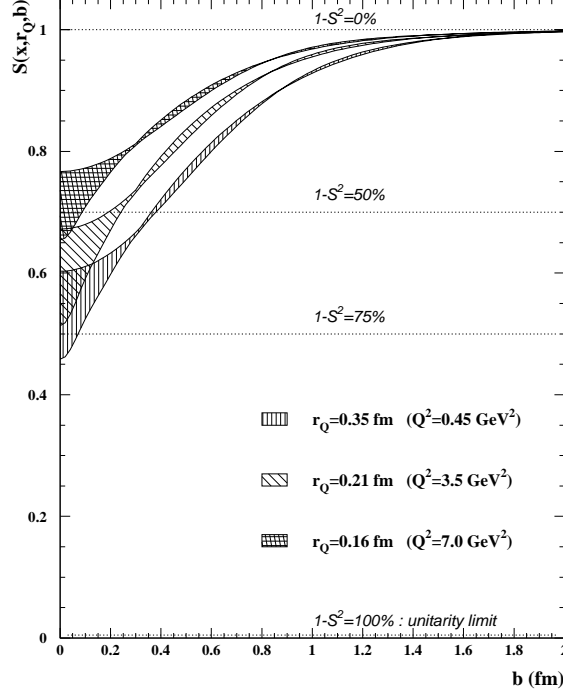


Fig. 9.  $S$ -matrix as a function of the impact parameter for  $x_{Bj} \sim 5 \cdot 10^{-4}$  and  $Q^2 = 0.45, 3.5, 7 \text{ GeV}^2$  (from [41]). The width of the bands represents the uncertainty due to the lack of experimental data for  $t > 0.6 \text{ GeV}^2$ . It is obtained by extrapolating the cross section with functions of  $t$  with behavior between  $t^{-3}$  and  $e^{-\lambda t}$ .

The linear DGLAP evolution equations are known to work well for inclusive structure function data. The saturation models incorporating non-linear contributions have thus to match this constraint. This uneasy problem has found in the conference two developments. The original saturation model [40] has been modified to take into account the linear evolution at small dipole size [42]. It indeed leads to a better description of  $F_2 \sim x_{Bj}^{-\lambda(Q^2)}$ , see [43]. Another proposal [44] is to match the linear and the non-linear behavior on the saturation critical line  $Q = Q_S(x_{Bj})$ . However, these proposals lead to modifications of the simple structure of the original model, *e.g.* the geometrical scaling behavior [44], which have to be confirmed/disproved by further phenomenological and theoretical investigations.

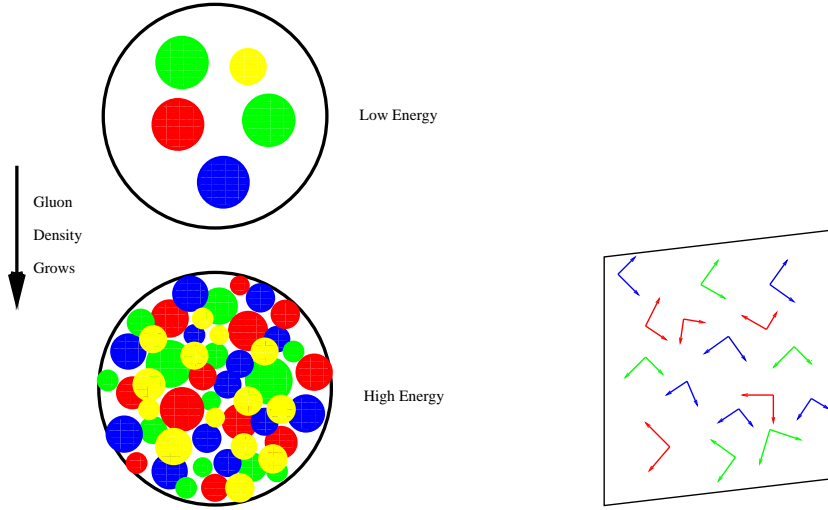


Fig.10. Saturation at small  $x_{Bj}$  and the “color glass condensate” (from [45]). Arrows schematically describe the classical QCD fields.

### 3.2.2. The Color Glass Condensate: a new QCD phase?

As we have seen, the evolution of the gluon distribution in a proton when  $x_{Bj} \rightarrow 0$  is expected to lead to an over-density in the geometrical phase space of the proton, see Fig. 10. The question arises then how to describe the new state with high density and weak coupling in QCD. A proposal has received the name “color glass condensate” [45]. The main idea is to consider that the abundance of gluons legitimates a classical colored field approximation (see Fig. 10). For each density increment due to the evolution to smaller  $x$ , new gluonic states are generated in the background of the classical field configuration. This gives rise to a non-linear evolution equation which can be interpreted as a high-density modification of the linear BFKL equation. The density increment is attributed either to an increase of nuclear size (*i.e.* a change of initial conditions) or to evolution towards small  $x_{Bj}$  (*i.e.* a change in the quantum evolution). This structure recently led to many applications such like geometrical scaling, saturation in hadron-hadron and heavy ion collisions, etc....

It would be interesting to disentangle, either theoretically or phenomenologically, the actual quantum evolution aspects from those coming from initial conditions. Another pending question is the relation, which has been recently advocated [45] (but also criticized [46]), between saturation and the Froissart bound. The Froissart bound comes from unitarity, analyticity and the existence of a “mass gap” in the theory, namely between zero and the

pion as the lowest mass state. This last requirement, related to confinement, is not apparent in the saturation picture.

### 3.3. Smallest- $x$ : the “Regge” mystery in QCD

Since a long time “Regge behavior” has been a great challenge for our understanding of high energy reactions. It mainly consists of  $2 \rightarrow 2$  particle amplitudes behaving as  $A^{el} \sim e^{\alpha_P(t) Y}$  for vacuum exchange reactions (also named *Pomeron*) and  $A^{inel} \sim e^{\alpha_R(t) Y}$  for various non vacuum quantum number exchanges (also named *Reggeons*). For soft hadronic reactions, the “Regge trajectories”  $\alpha_{P,R}(t) \sim \alpha_{P,R}(0) + \alpha'_{P,R} t$  are thus found to be phenomenologically linear, with universal intercepts  $\alpha_{P,R}(0)$  and slopes  $\alpha'_{P,R}$  for a given set of exchanged quantum numbers. Since long, there are attempts to derive the Regge behavior from resummation of the perturbative QCD expansion at large  $Y$ , while, recently, new tools for non-perturbative QCD estimates have been experienced. Note that the “Regge behavior” has become even more mysterious by the experimental evidence for the  $Q^2$ -dependence of effective intercepts and slopes for hard  $2 \rightarrow 2$  processes, such as  $\gamma^* p$  cross-sections.

#### 3.3.1. The origin of “Regge behavior” in pQCD

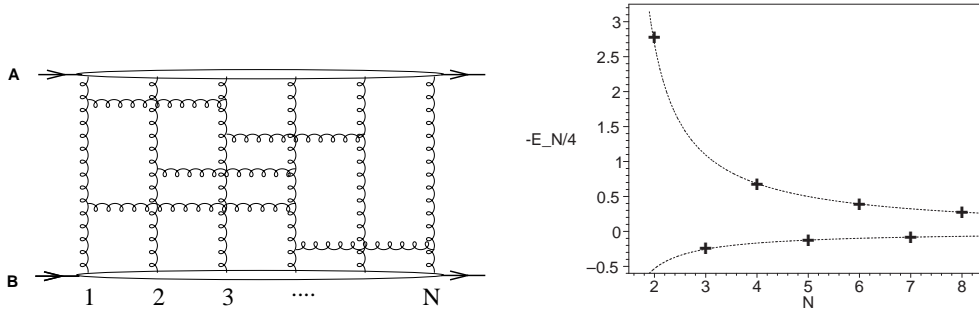


Fig. 11. Feynman graphs and dependence of the intercept  $\epsilon_N$ , on the number of gluon ladder up-rights  $N$  (from [47]).

On the pQCD side of the question, the challenge is to sum Feynman diagrams contributing to the large  $Y$  behavior of amplitudes. Generalizing those of Fig. 7, with 2 gluon up-rights corresponding to the BFKL equation, one needs to resum those of Fig. 11 with  $N$  gluon up-rights (and gluon rungs connecting any two of them), which is a formidable task. In fact, a solution for intercepts has only now been found [47] and reported at the conference. The mathematical breakthrough was the recent formulation of the problem

as an integrable quantum spin chain with  $N$  sites and ground energies  $\epsilon_N$ . However from “integrable” to “integrated” required a lot of work. As a result, one obtains a series of intercepts  $\alpha_N(0) \equiv \frac{g^2 N_c}{4\pi} \epsilon_N$  which, for an even number of gluon up-rights (see Fig. 11), contribute to the *Pomeron* sector, while for an odd number of gluon up-rights, contribute to the elusive *Odderon* which has not been yet found experimentally. Interestingly enough, all Pomeron intercepts are greater than 1 (growing contributions to total cross-sections), while all Odderon ones are less than 1. Note however another solution [48] with Odderon intercepts equal to one. These theoretical investigations should lead to a deeper understanding of the connection of the Regge behavior with QCD. For instance the couplings of external sources, and the dependence on the hard scale (which is fixed in actual calculations) are both problems to be addressed soon. Summing non planar diagrams which are known to contribute is yet another deep challenge.

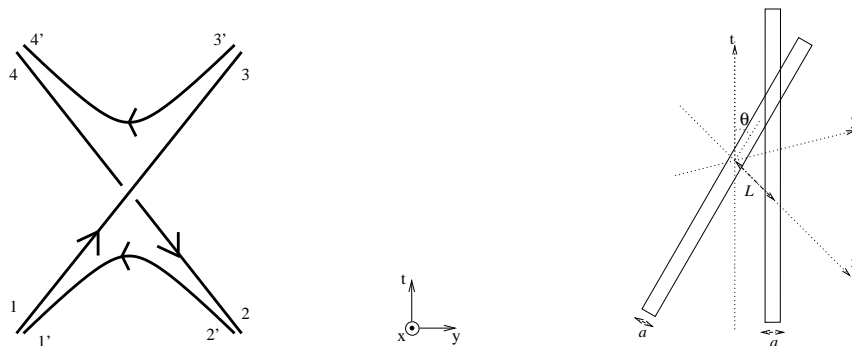


Fig.12. *Boundaries of Minimal surfaces for Reggeon and Pomeron amplitudes (from [49]).*

### 3.3.2. The origin of “Regge behavior” in non-pQCD

Even a more formidable challenge is the origin of the Regge behavior in reactions where it has been displayed by data, *i.e.* soft reactions corresponding to the unknown strong coupling regime of QCD. While phenomenological work may still be needed [50], new tools of handling non perturbative calculations for strongly coupled gauge theories have been investigated. Using the new duality properties relating strongly coupled gauge theories to weakly coupled string theories in a non-flat background space called *AdS/CFT* duality, the Pomeron and Reggeon amplitudes have been related [49] to a particular geometrical problem: finding minimal surfaces corresponding to specific boundary conditions, see Fig. 12. In this frame-

work, “Reggeization”, *i.e.* linearly rising Regge trajectories, is related to the string background metrics in much the same way as confinement is related to the Wilson loop area law.

The obtained values of Pomeron and Reggeon intercepts and slopes are in the correct range, but some approximations in the calculation have to be improved to get more precise results. The connection of *AdS/CFT* duality with quantum field theory features (such as instantons, solitons) is highly desirable, the most difficult problem being the identification of the supergravity dual of QCD in a generalized AdS/CFT correspondence. Despite these difficulties, this new approach appears quite promising.

### Acknowledgments

This paper is dedicated to the memory of Bo Andersson, who died unexpectedly from a heart attack on March 4th, 2002. We all have learned so much from him.

We want to thank the organisers for this nice and well prepared workshop and also all the participants of our working group sessions for their contributions and the lively discussions.

### REFERENCES

- [1] P. Laycock, these proceedings and references therein
- [2] F. P. Schilling, 2002, private communication.
- [3] F. P. Schilling, these proceedings and references therein
- [4] M. Capua, these proceedings and references therein
- [5] K. Borras, these proceedings and references therein
- [6] A. Levy, these proceedings and references therein
- [7] K. Klimek, these proceedings and references therein
- [8] X. Janssen, these proceedings and references therein
- [9] D. Brown, these proceedings and references therein
- [10] A. Airapetian, these proceedings and references therein
- [11] R. Stamen, these proceedings and references therein
- [12] A. Freund, these proceedings and references therein
- [13] T. Berndt, these proceedings and references therein
- [14] R. Heremans, these proceedings and references therein
- [15] V. Simak, these proceedings and references therein
- [16] K. Terashi, these proceedings and references therein
- [17] DØ Collaboration, Proposal for a Forward Proton Detector at DØ Fermilab PAC, 1997.



- [18] K. Goulianos, these proceedings and references therein
- [19] A. D. Roeck, C. Royon, these proceedings and references therein
- [20] A. Martin, these proceedings and references therein
- [21] M. Boonekamp, these proceedings and references therein
- [22] N. Timneanu, R. Engberg, G. Ingelman, these proceedings and references therein
- [23] A. Bialas, these proceedings and references therein
- [24] P. Newman, these proceedings and references therein
- [25] A. Caldwell, these proceedings and references therein
- [26] A. Kyrieleis, these proceedings and references therein
- [27] L. Lönnblad, these proceedings and references therein
- [28] N. Vlasov, these proceedings and references therein
- [29] P. Thompson, these proceedings and references therein
- [30] C. Adloff et al., *Eur. Phys. J. C* **20** (2001) 29, hep-ex/0012051.
- [31] C. Adloff et al., *Phys. Lett. B* **520** (2001) 191, hep-ex/0108047.
- [32] L. Schoeffel, these proceedings and references therein
- [33] R. Engberg, these proceedings and references therein
- [34] I. Ivanov, N. Nikolaev, these proceedings and references therein
- [35] R. Sandapen, these proceedings and references therein
- [36] M. McDermott, these proceedings and references therein
- [37] D. Schildknecht, these proceedings and references therein
- [38] A. Utermann, these proceedings and references therein
- [39] S. Goloskokov, these proceedings and references therein
- [40] K. Golec-Biernat, these proceedings and references therein
- [41] S. Munier, these proceedings and references therein
- [42] K. Golec-Biernat, these proceedings and references therein
- [43] V. Chekelian, A. Cooper-Sakar, R. Thorne, these proceedings and references therein
- [44] J. Kwiecinski, A. Stasto, these proceedings and references therein
- [45] L. McLerran, these proceedings and references therein
- [46] A. Kovner, U.A. Wiedemann, these proceedings and references therein
- [47] J. Kotanski, these proceedings and references therein
- [48] H. de Vega, L.N. Lipatov, these proceedings and references therein
- [49] R. Janik, these proceedings and references therein
- [50] A. Vinnikov, these proceedings and references therein